PERGAMON

International Journal of Heat and Mass Transfer 41 (1998) 2867–2875

International Journal of HEAT and MASS TRANSFER

Transient convective heat transfer in a helical coiled tube with pulsatile fully developed turbulent flow

Liejin Guo,* Xuejun Chen, Ziping Feng, Bofeng Bai

State Key Laboratory of Multiphase Flow in Power Engineering, Xi'an Jiaotong University, 710049 Xi'an, Shaanxi, China

Received 23 January 1998

Abstract

Experiments were conducted to investigate the effects of pulsation upon transient heat transfer characteristics for fully-developed turbulent flow in a uniformly heated helical coiled tube. The non-uniform feather of local heat transfer with steady flow was also examined. The secondary flow mechanism and the effect of interaction between the flow oscillation and secondary flow were analyzed on the basis of the experimental data. Some new phenomena were observed and explained. A series of correlations were proposed for the average and local heat transfer coefficients both under steady and oscillatory flow conditions. The results showed that there were considerable variations in local and peripherally time-average Nusselt numbers for pulsating flow in a wide range of parameters.

Nomenclature

a excitation parameter for oscillatory flow in ref. [13]
A_p oscillatory amplitude [kg m^{-2}]
C_p specific heat [kJ m^{-3} °C]
d inner diameter of tube $d = 2r$ [m]
D coil diameter, $D = 2R$ [m]
f frequency of oscillation [1 s^{-1}]
G mass flow rate [kg m^{-2}]
h heat transfer coefficient [kJ m^{-2} °C]
i, j, k grid number of space
K thermal conductivity [W m °C^{-1}]
m grid number of time
Nu $h \cdot d/k$, local Nusselt number
P pressure, [Pa]
q heat flux [kW/m^{-2}]
Re Reynolds number
r the radial coordinate [m]
R radius of coils [m]
t time [s]
T temperature [°C, K]
S interior heat source [W m^{-3}]
Y measurement value of wall temperature [°C].

Greek symbols
θ the coordinate for the peripheral angle
μ fluid dynamic viscosity [kg m^{-2} s^{-1}]
ρ fluid density [kg m^{-2}]
ϕ sensitivity coefficient.

Subscripts
c coil average
f fluid
I inner
l liquid phase
osc oscillatory
p peripheral point of cross section
s cross-sectional average.

1. Introduction

Helically coiled tubes are utilized extensively for piping systems of oil pipelines, heat exchangers, steam generators and chemical plants, etc., because of their practical importance of high efficiency in heat transfer, compactness in structure, ease of manufacture and arrangement. Horizontal direction of tube axis is an attractive orientation due to its lower gravitation center and higher efficiency both in heat transfer and steam generation. For these reasons it also is favored for space,

* Corresponding author. Tel.: ++86 29 3268767; fax: +86 29 3237910; e-mail: lj-guo@sun20.xjtu.edu.cn.

0017-9310/98 $19.00
PII: S0017-9310(97)000376-1

navigation and other special techniques. Pressure for intensification has driven increased demand for improved understanding of the key mechanisms responsible for fluid flow and heat/mass transfer encountered in these devices [1, 2].

For internal flow of curved pipes, many investigations have been performed in practical use and many theoretical and experimental results have been reported. However, most of them were concerned with steady flows [3–5]. On the other hand, studies have become more important on unsteady or pulsating flows at the start–stop or the undesirable accident of pumps, blowers and other equipment because recent fluid turbo-machinery has larger scales and faster transfer rate. Also in the field of bio-engineering, great attempts have been made to solve problems concerning blood circulation through a heart and an artery from the viewpoint of hydraulics. An increasing amount of attention to problems of unsteady fluid mechanics and heat mass transfer has been seen in the last thirty years. Some important examples that have been successfully tackled include rocket combustion instabilities and unsteady atmospheric re-entry, while continuing challenges include the possibility of improving the efficiency of heat exchangers [1, 6–10].

In some instances it may even be beneficial to induce pulsation in flow systems if enhanced performance will ensue. However, not many reports have been published on unsteady pipe flow, especially on unsteady flow in curved tubes. Only a few results have been reported because of its complicated phenomena.

Lyne [9] initiated the analysis of unsteady pulsatile flow in curved tubes. The motion induced in a circular tube by a sinusoidally time-vary pressure gradient with zero mean is assessed. He predicted additional secondary circulation of opposite direction to that of steady flow in the inviscid core, and postulated that this additional secondary flow is due to shear action. Zalosh and Nelson [11] used the finite Hankel Transform to obtain analytical solution for a medium range of the frequency parameter a. For a wider range of a, Chow and Li [12] employed the same technique used by Zalosh and Nelson to find that the secondary flow pattern vary with respect to a and can be divided into three distinct phases dictated by the relative importance of the viscous and inertial forces: (1) the shear force dominated flow with single circulation; (2) the transitional flow with either one or two circulations; (3) the boundary layer flow with either one or two circulations. They confirm Lyne's prediction of the formation of an additional circulation in the inviscid core but they report that it is more likely to be due to the inertial forces rather than the shear action as postulated by Lyne [9].

Simon et al. [13] used a perturbation analysis including the second order solution for flow and heat transfer under small Dean number ($Dn < 22$) and a wide range of excitation parameters ($a = 0.1$–$1.2, k = 0.01$–3), Prandtl number ($Pr = 1.0$–100). Their results show that the increase in time average Nusselt number is most evident at high Prandtl numbers, high excitation relative amplitudes and low excitation frequencies. They reported that the Nusselt number ratio (curved pulsatile to straight pulsatile) passes through a maximum value at low a. This unusual result was negated by the more exact numerical solution results described in their follow up paper [14]. It can be inferred that perturbation analyses, limited as it is to solution of the second-order, is unable to model accurately the complicated secondary flow phenomena in pulsatile flow especially at low excitation frequency. Up to now, the solutions for pure oscillatory and pulsatile flows available in the literature are mostly analytical (restricted to $Dn < 22$) or numerical (restricted to laminar flow). Conflicting results have been reported for the pulsating flow and heat transfer in straight tubes. In some cases the flow pulsation seem to enhance the heat transfer, whereas, in other cases either no significant effect is shown or a decrease occurs [8, 15, 16]. A detailed knowledge of the flow and heat or mass transfer phenomena in such cases could lead to improved performance in the design of engineering equipment.

The purpose of the present study is to examine the secondary flow mechanisms experimentally by extending the range of Dn to turbulent flow, and to show the outcome of the interaction between the flow oscillations and secondary flow. The effects of this interaction on heat transfer is made clear by nondimensional parameter Nu, Dn, Re, and two new excitation parameters of oscillation. such as the Wormersly number for oscillatory frequency, Wo, and the ratio of oscillatory amplitude, A_p. The results show that there is considerable variation in local and average Nusselt number. A series of new correlations are proposed for the distribution of local heat transfer coefficients and their average value under steady turbulent flow, and for the time and cross peripheral average heat transfer coefficients under unsteady or oscillatory turbulent flow.

2. Experimental apparatus and procedure

2.1. Experimental apparatus

The experiment was conducted in a closed-cycle test loop of steam water two phase flow. The loop is schematically illustrated in Fig. 1. It was constructed of a centrifugal pump to supply power for the fluid flow, a pressurized nitrogen tank to maintain and control the system pressure, a series of orifices to measure water mass flow rate, a pre-heater to heat fluid and control the inlet temperature, a test section, a water cooled condenser and a water tank. The resistance of the tube wall of both test section and pre-heater was used to heat the working fluid

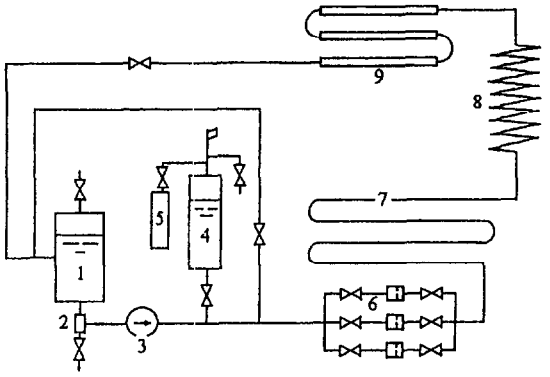

Fig. 1. The closed circulation steam–water two-phase flow test loop.

with alternating electrical current delivering total power of 200 kw.

The test section was made of a 6448 mm long tube of $\phi 15 \times 2$ mm, with helix angle of 4.27°, coil diameter of 256 mm and a pitch of 60 mm, as shown in Fig. 2. It was thermally insulated by wrapping with fiberglass. The mass flow rate of working fluid through the test section was measured by using three orifice meters in different ranges (in house construction with standard specification) appending to three differential pressure transducers (Model 1151 DP, Xi'an Instrument and Meter Plant, a cooperation enterprise jointly with U.S.A.) with response time of 0.1 s. Two manometers were used to measure the pressure at the inlet and outlet of the test section. The pressure drop of the test section measured by a differential pressure transducer. Three armoured thermocouples (made of NiCr and NiSi wires with 1 mm diameter) were installed into the core of the tube to measure the fluid temperature of inlet, central station and outlet of test section. One hundred and two thermocouples (made of NiCr and NiSi wires with 0.3 mm diameter) were installed on the outer surface of the heated tube wall to measure the temperature of the wall, eight were arranged uniformly along the periphery of the outer surface of the tube wall one at each cross-section of every quarter turn among the first, second and third turns of coils, all of them were attached to the tube wall and electrically insulated so that the effect of heating electrical current on it was avoided.

All of the instantaneous signals of parameters and the input powers of heat to test section and pre-heater were monitored and stored on an IBM PC computer via six isolated measurement pods, and also recorded and monitored by an AR-5000 cassette tape recorder so that further statistical analysis could be done on some runs. The system for parameter measurement and collection is shown in Fig. 3.

2.2. Experimental procedure

Preliminary experiments of steady single phase flow and heat transfer were performed to verify the reliability of the experimental system. The experimental results showed good agreement with the pressure drop correlation by Ito et al. [17], and with the average heat transfer coefficient correlation by Seben and Mclaughlin [18] as follows:

$$Nu_c = 0.023 Re^{0.8} Pr^{0.4} [Re(d/D)^2]^{0.05} \quad \text{for } 6000 < Re < 60\,000 \quad (1)$$

steady-state characteristic of the system were obtained in terms of pressure drop vs. mass flow rate and were used to locate instability boundaries and determine the steady

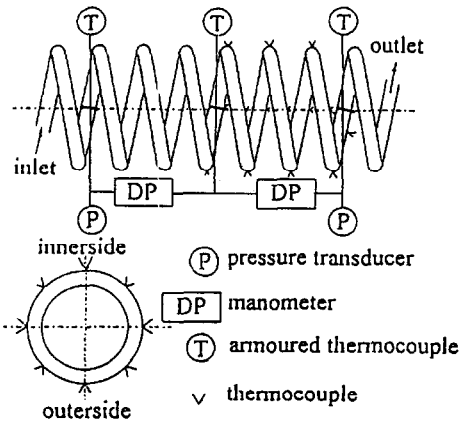

Fig. 2. Test section and the arrangements of probes, transducers and thermocouples.

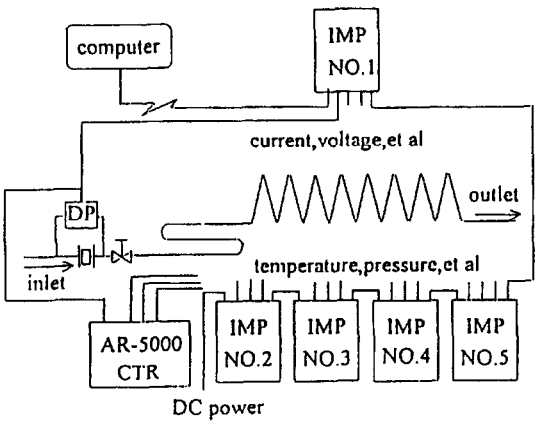

Fig. 3. Diagram of measurement and data collection system.

and unsteady regions for the following range of parameters:

System pressure	$P = 0.5$–3.5 MPa
Mass flow rate	$G = 150$–2500 kg m^{-2} s^{-1}
Heat flux	$Q = 0$–540 kW m^{-2}.

The tests were conducted using the following procedure:

(1) Establish and operate parameters including the mass flow rate, compressible volume, and inlet temperature, and confirm their good stability.
(2) Increase the heat flux of test section and await establishment of thermal equilibrium or; if unstable, await sustained oscillation, recording the average value of the system parameters and oscillatory records over two or more periods.
(3) Repeat these procedures after adjusting the operating parameters.

3. Data reduction

In order to calculate the heat transfer coefficients, the temperature and heat flux values on the inner surface of the tube and the bulk temperature of working fluid need to be determined beforehand. Here the numerical solutions developed by the present authors [19, 20] were employed.

For steady flow, a solution for the nonlinear two-dimensional inverse problem of heat conduction about the tube wall of helical coils was used on the assumption that: (1) the longitudinal heat conduction was small and can be neglected; (2) the interior heat source was uniformly distributed and (3) the thickness of tube wall was taken to be a constant [19].

The heat conduction equations and boundary conditions used were as follows:

$$\nabla(K\nabla T)+S=0 \tag{2a}$$

$$\frac{\partial T}{\partial r}=0; \quad \text{for } r=r_0 \tag{2b}$$

$$k\frac{\partial T}{\partial r}=h(\theta)\cdot(T_w-T_f); \quad \text{for } r=r_i \tag{2c}$$

$$T(r,\theta)=Y_i, \quad i=1,2,\ldots,N_T; \quad \text{for } r=r_0 \tag{2d}$$

where $h(\theta)$ is the unknown heat transfer coefficient; which is discrete as $(h_1, h_2, \ldots, h_{N_T})$; N_T, the total number of thermocouples arranged on one cross-section; Y_i, the measured value of the ith thermocouple on one cross-section.

If $h(\theta)$ was obtained the sum of the $\Sigma(T(r_0,\theta_i)-Y_i)^2$ was the minimum, therefore the following equation is tenable

$$\sum_{i=1}^{N_T}[T(r_0,\theta_i)-Y_i]\frac{\partial T}{\partial h_k}=0, \quad k=1,2,\ldots,N_T. \tag{3}$$

The bulk temperature of fluid is determined by using thermal equilibrium and linear pressure differential gradient assumption along the flow direction in a single phase region.

The mean heat transfer coefficient of the ith cross-section $\bar{h}_{si}$ and that of the whole coils $\bar{h}_c$ are calculated by the following methods:

$$\bar{h}_{si}=\frac{\bar{Q}_{si}}{\bar{T}_{wk}-T_f} \tag{4a}$$

$$\bar{q}_{Si}=S\cdot 2\pi r_i \tag{4b}$$

$$\bar{T}_{Wi}=\frac{1}{N_T}\sum_{k=1}^{N_T}T(r_i,\theta_k) \tag{4c}$$

$$\bar{h}_c=\frac{1}{N_s}\sum_{i=1}^{N_s}\bar{h}_{si} \tag{4d}$$

where N_s was the total number of the calculated cross sections.

For unsteady or pulsatile flow, the transient local heat transfer coefficients were obtained by solving a multi-dimensional transient inverse heat conduction problem using a least-square method developed by the present authors [20].

The mathematical model for this problem was used as follows:

$$\rho c_p\frac{\partial T}{\partial t}=\frac{1}{r\omega}\left[\frac{\partial}{\partial r}\left(\left(kr\omega\frac{\partial T}{\partial r}\right)+\frac{\partial}{\partial\theta}\left(k\frac{\omega}{r}\frac{\partial T}{\partial\theta}\right)\right]+S \tag{5a}$$

$$-k\frac{\partial T}{r\,\partial\theta}=h(\theta,t)(T-T_\infty), \quad r=r_0 \tag{5b}$$

$$-k\frac{\partial T}{r\,\partial\theta}=q(\theta,t), \quad r=r_i \tag{5c}$$

$$T=T_0(r,\theta), \quad t=0 \tag{5d}$$

$$T_i(r,t)=Y_i(t), \quad i=1,2,\ldots,N_m, \quad r=r_0 \tag{5e}$$

where $\omega=1+R\cdot r\cdot\sin\theta/(R^2+P^2)$; $Y_i(t)$ is the measured value of the ith thermocouple at the instant t; $h(\theta,t)$ is the known heat transfer coefficient on outer surface of tube wall and a function of time. $q(\theta,t)$ is the unknown heat flux on inner surface of tube wall, which need to be solved. The procedure for the simultaneous determination of all of the q_m values describing $q(\theta,t)$ it as follows:

(1) Assume $Q(\theta,t)$ is the result of nonlinear estimation, one minimizes the following sum of squares function

$$J(\ddot{q}_M)=\sum_{i=1}^{N_m}[T_{i,M}-Y_{i,M}] \tag{6}$$

where $\ddot{q}_M$ is a vector of unknown heat flux on inner surface of tube wall $(q_1, q_2, \ldots, q_M)$, at the instant t_M, i.e., the mth step of time.

(2) According to the theory about extreme value of function, one can obtain

$$2\Sigma(T_{i,M}-Y_{i,M})\frac{\partial T_{i,M}}{\partial q_{k,M}}=0,\quad k=1,2,\ldots,N_m \tag{7}$$

where $T_{i,M}$ would be represented by Taylor series approximation of $T_{i,M-1}$, $q_{i,M-1}$ and $q_{i,M}$ as follows:

$$T_{i,M}=T^*_{i,M}+\sum_{j=1}^{N_m}\frac{\partial T_{i,M-1}}{\partial q_{j,M-1}}(q_{j,M}-q_{j,M-1}) \tag{8}$$

where, $T^*_{i,M}$ is the value of T estimated by using only the value of $T_{i,M-1}$, and $\ddot{q}_{M-1}$ at the former step of time t_{M-1}, the partial derivative in equation (8), $\partial T_{i,M-1}/\partial Q_{j,M-1}$ is frequently called as a sensitivity coefficient, $\phi_{i,j,m}$.

Introducing equation (8) into (7), one obtains

$$\sum_{i=1}^{N_m}(T^*_{i,M}-Y_{i,M})\phi_{i,R,M}+\sum_{i=1}^{N_m}\sum_{j=1}^{N_m}\phi_{i,k,m}\phi_{i,j,M}(q_{j,M}-q_{j,M-1})=0. \tag{9}$$

Taking a particle derivative of $q_{j,M}$ from the two sides of equation (9), one derives the solution equation for sensitivity coefficients as follows:

$$\frac{1}{r\omega}\left[\frac{\partial}{\partial r}\left(kr\omega\frac{\partial\phi_{j,M}}{\partial r}\right)+\frac{\partial}{\partial\theta}\left[k\frac{\omega}{r}\frac{\partial\phi_{j,M}}{\partial\theta}\right]\right]=\rho c_p\frac{\partial\phi_{j,M}}{\partial t} \tag{10a}$$

$$-k\frac{\partial\phi_{j,M}}{\partial\theta}=h(\theta,t)\phi_{j,M},\quad r=r_0 \tag{10b}$$

$$-k\frac{\partial\phi_{j,M}}{r\,\partial\theta}=\delta_{i,j},\quad r=r_i \tag{10c}$$

$$\delta_{i,j}=1\quad(i=j,j=1,2,\ldots,N_m)$$
$$\delta_{i,j}=0\quad(i=j,j=1,2,\ldots,N_m)$$
$$\phi_{j,M}=0,\quad t=t_{m-1}. \tag{10d}$$

where, $\phi_{j,M}$ is the sensitivity coefficient of temperature $T_{j,M}$, to heat flux q_j at the instant of t_m.

Using the temperature and thermal physical properties at former step t_{m-1}, one can solve the equation (10) to obtain the sensitivity coefficients, then solve equation (9) to get the values of unknown boundary conditions. Finally, solve the normal heat conduction problem of tube wall to get the temperature field at t_M time step. The mean heat transfer coefficients of one cross-section and whole coils at the instant t_M can be calculated by similar method to equation (4), and the time-averaged values were calculated by the following method.

$$\bar{A}=\frac{1}{T}\int_0^T A(t)\,dt\quad\text{or}\quad\bar{A}=\frac{1}{N_t}\sum_{m=0}^{N_t}A(t) \tag{11}$$

where $N_t=n_p\cdot T/\Delta T$; T is the period of the oscillation; Δt is the time step for numerical discrete, n_p is the number of period of data being cut off for calculating of time-average value, M is an integer.

4. Experimental results and discussion

4.1. Turbulent heat transfer for steady flow

4.1.1. Average heat transfer coefficient

As mentioned in Section 2, the average heat transfer coefficient in developed turbulent flow in helical coiled tubes may be calculated by equation (1) when $Re<60\,000$. Our experimental results showed good agreement with equation (1) verifying the reliability of our experiments. When $Re>60\,000$, equation (1) cannot be used. As shown in Fig. 4, our experimental data were found to be located between the predicted curve by equation (1) and the correlation curve by Dittus–Boelter for straight tubes. A new correlation was developed and proposed for a wider range of Reynolds number as follows:

$$\overline{Nu}_c=\frac{\bar{h}d}{k}=0.328Re^{0.58}Pr^{0.4}\quad 6000<Re<180\,000 \tag{12}$$

where the characteristic temperature is defined as the bulk temperature of working fluid T_f, and a reasonable agreement is reached within $\pm9.2\%$ derivation between the calculated value and experimental data.

It is seen from the figure that with increasing Re to higher level, the average heat transfer coefficient for coils tends to coincide with the correlation for straight tubes. This phenomenon was not reported in previous investigations because the Reynolds number encountered in the previous investigations did not reach such a higher level. This trend implies that at very high Reynolds number the effect of secondary flow in helical coiled tubes on the enhancement heat transfer become less significant due to thinning of the thermal boundary layer.

4.1.2. Longitudinal cross-sectional average heat transfer coefficient

As the coil is orientated horizontally, the angle between the gravity force and flowing direction changes con-

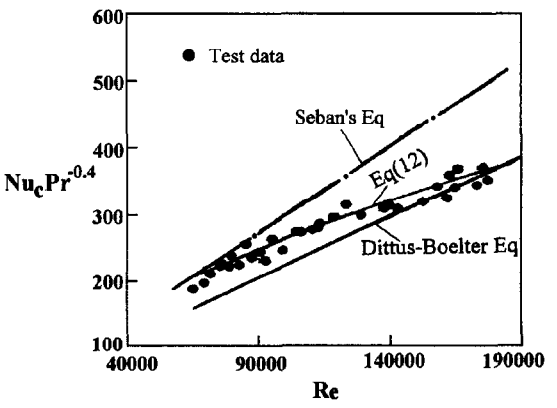

Fig. 4. Test results on the average turbulent heat transfer.

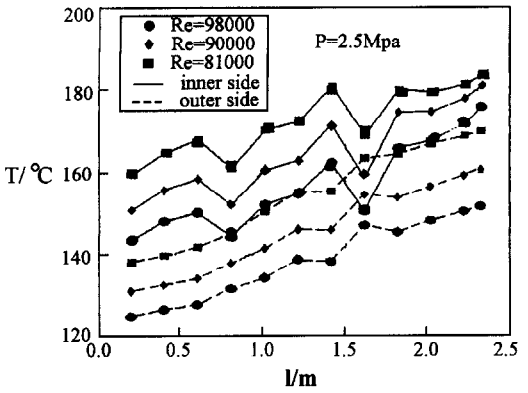

Fig. 5. Local wall temperature along the tube axial direction.

tinuously and periodically, the flow velocity distribution in radial direction on each cross-section varies also periodically along longitudinal axial direction of coils and the heat transfer rates do similarly. Figure 5 illustrates the results of measurements about the wall temperature distribution along the helical axial direction there is a periodical feature and the lower value at the cross-section on which fluid flow upwardly in tube. In the form of $\overline{Nu_s}/\overline{Nu_c}$, the distribution of average heat transfer coefficient corresponding to that of wall temperature is shown in Fig. 6 and also have a good periodical feature.

The average heat transfer coefficients in the upward flow region of coils are higher than those in the downward flow region and 120–130% of the average value of total coils. The reason may be that the gravity force acts as a drag force for the upward flow and lead boundary layers near the wall of the tube to become thinner and the distribution of flow velocity in radial direction to become mean. Therefore it is unreasonable to use the cross-sectional average heat transfer coefficient at the outlet as the average value of total coils, which frequently was used before.

4.1.3. Peripheral local heat transfer coefficients

The experimental data of the distribution of local heat transfer coefficient along the peripheral angle θ are shown in Fig. 7 in the form of relative value Nu_p/Nu_s. The peripheral local heat transfer coefficient takes its largest value on the outside which is about 1.6–2.2 times the cross-sectional average value, while it has its smallest one on the inner side which is half of the average value and has the average value on the top and bottom side. With increasing $Re\,Pr$, Nu_p/Nu_s becomes greater on the outside, but keep constant on the inner side. This phenomena was also observed by Seban et al. [18]. This is nearly symmetry and can be correlated by

$$\frac{Nu_p}{Nu_s} = 022\left(\frac{Re\,Pr}{10^4}\right)^{0.45}(0.5+0.1\theta+0.2\theta^2). \tag{13}$$

These imply that the secondary flow pattern in coils exists nearly symmetry circulations in steady single phase turbulent flow.

4.2. Unsteady oscillatory heat transfer

4.2.1. Time average heat transfer coefficient The other motivation for this work is derived from the conclusions of a previous analytical and experimental investigation of thermo-hydrodynamic instabilities encountered in boiling channels. The prediction of the threshold of stability by the analytical model requires more accurate understanding and knowledge of the radial and axial heat conduction and diffusion effects in the single phase region of the flow channel which affect the axial propagation of enthalpy perturbation, and of the effect of thermal non-equilibrium, i.e., subcooled boiling [21, 22]. There is promising but somewhat limited evidence that this results in a better analytical prediction of experimental system

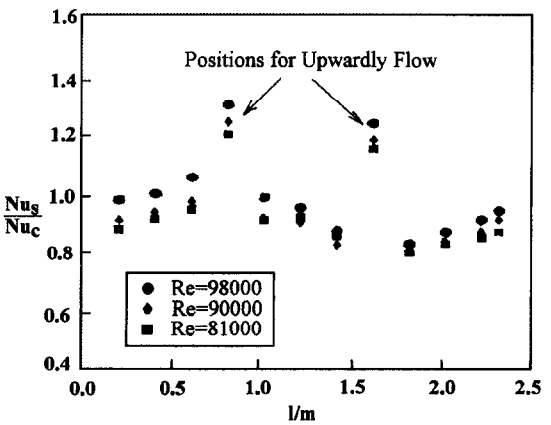

Fig. 6. Local turbulent heat transfer coefficient along the tube axial direction.

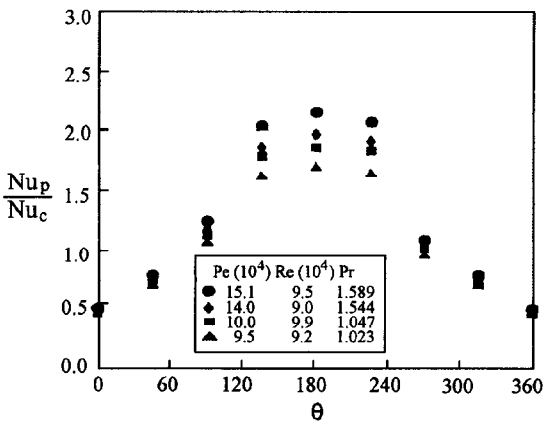

Fig. 7. Peripheral local turbulent heat transfer coefficient on the outlet cross-section.

stability limits when above effects are incorporated in the dynamic model of a boiling system [21, 22]. No systematic study of these effects exists in the literature.

The experimental work reported here is to study the characteristics of heat transfer with oscillatory turbulent subcooled flow corresponding to thermal hydrodynamic oscillations encountered in boiling channels.

Figure 8(a)–(c) shows the experimental results of the time and cross-section averaged heat transfer coefficients for oscillatory single phase turbulent flow, and comparisons with some correlation [18, 23] for steady flow, and the variation characteristics of oscillatory heat transfer coefficient with the changes of oscillatory frequency number Wo and the ratio of oscillatory amplitude $\bar{A}_p$.

The data of oscillatory heat transfer coefficients are totally higher than that of steady flow with corresponding conditions, obviously, oscillations enhance the single phase turbulent heat transfer, and the enhancement of effects of oscillations increase with increasing time-averaged Reynolds number Re, as shown in Fig. 8(a).

As more important features about oscillation heat transfer which can be observed from Fig. 8(b) and (c) is that there exists a strong dependence on oscillatory frequency and amplitude. Here we introduce two non-dimensional parameters to represent their influence, which is defined, respectively, as follows:

The oscillatory frequency number Wo:

$$Wo = d\sqrt{2\pi f/\mu_l}. \tag{14}$$

The ratio of oscillatory amplitude $\bar{A}_p$.

$$\bar{A}_p = \frac{(G_{max} - G_{min})}{2G_0} \tag{15}$$

where $\bar{G}_0$ is the time averaged mass flow rate; and G_{max}, G_{min} is the maximum and minimum value of mass flow rate in an oscillatory period, respectively; f is the frequency of oscillation.

The $\overline{Nu}_{osc}$ decreases sharply with increasing Wo in the range of $Wo \leqslant 5.5$, and maintains approximately fixed in the range of $Wo > 5.5$. This means that the oscillation in a low frequency is more beneficial for heat transfer enhancement than that in high frequency.

The influence of $\bar{A}_p$ can also be divided into two regions, when $\bar{A}_p < 1.5$, $\overline{Nu}_{osc}$ keep nearly a constant; when $\bar{A}_p \geqslant 1.5$, $\overline{Nu}_{osc}$ increases gradually with increasing $\bar{A}_p$, the larger amplitude of oscillation will enhances heat transfer.

Based on the experimental data, the time-average heat transfer coefficient of helical coils with oscillatory single phase turbulent flow can be correlated in the following form

$$\overline{Nu}_{osc} = 0.147\overline{Wo}^{-0.31} Pr^{-4.4}\left(\frac{\overline{Dn}}{1000}\right)^{0.82} \tag{16}$$

the above equation is applicable for the range of oscillatory $f = 0.05$–0.003, $\overline{Re} = 25\,000$–$125\,000$, and a reasonable agreement is reached within $\pm 15\%$ derivation between the calculated value and experimental data.

4.2.2. *Transient local heat transfer coefficients and their phase lag*

Figure 9(a)–(c) reports the records of the process of a flow rate oscillation and corresponding variations of transient local heat transfer coefficient in a period, where $t = 21.8$–24.8 s is corresponding to the part of the period of flow rate increasing and $t = 26.7$–37.6 s is the part of flow rate decreasing. The local heat transfer coefficient h_{osc} has a reverse phase angle characteristics relative to the phase characteristic of flow rate oscillation, that is, it decreases with increasing flow rate G, when G reaches the maximum, h_{osc} becomes minimum, and vice verse.

The distribution of transient local heat transfer coefficients in peripheral angle θ direction become non-uniform and asymmetrical, its smallest value always occurs at the inner side ($\theta = 0°$) and largest one does at the position of circumferential angle $\theta = 135°$ approximately. With increasing flow rate, the h_{osc} tends to uniform in the one cross-section, there exists one peak during

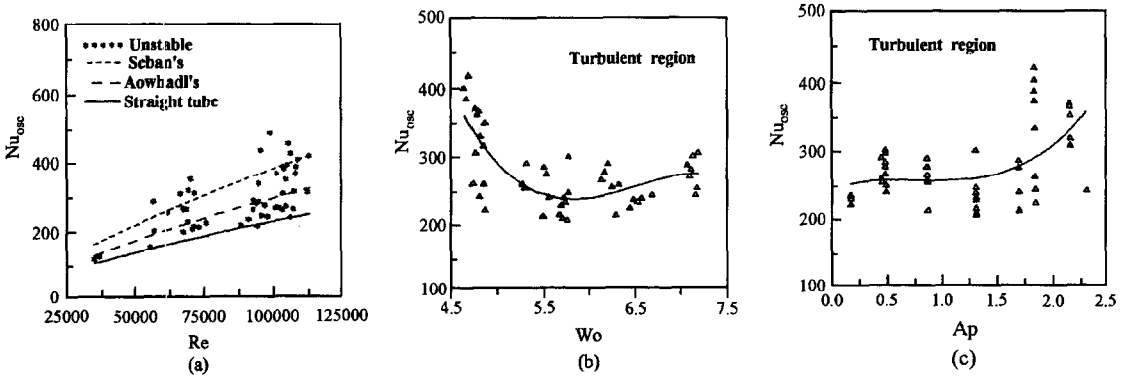

Fig. 8. Experimental results of averaged heat transfer coefficients for oscillatory single phase turbulent flow.

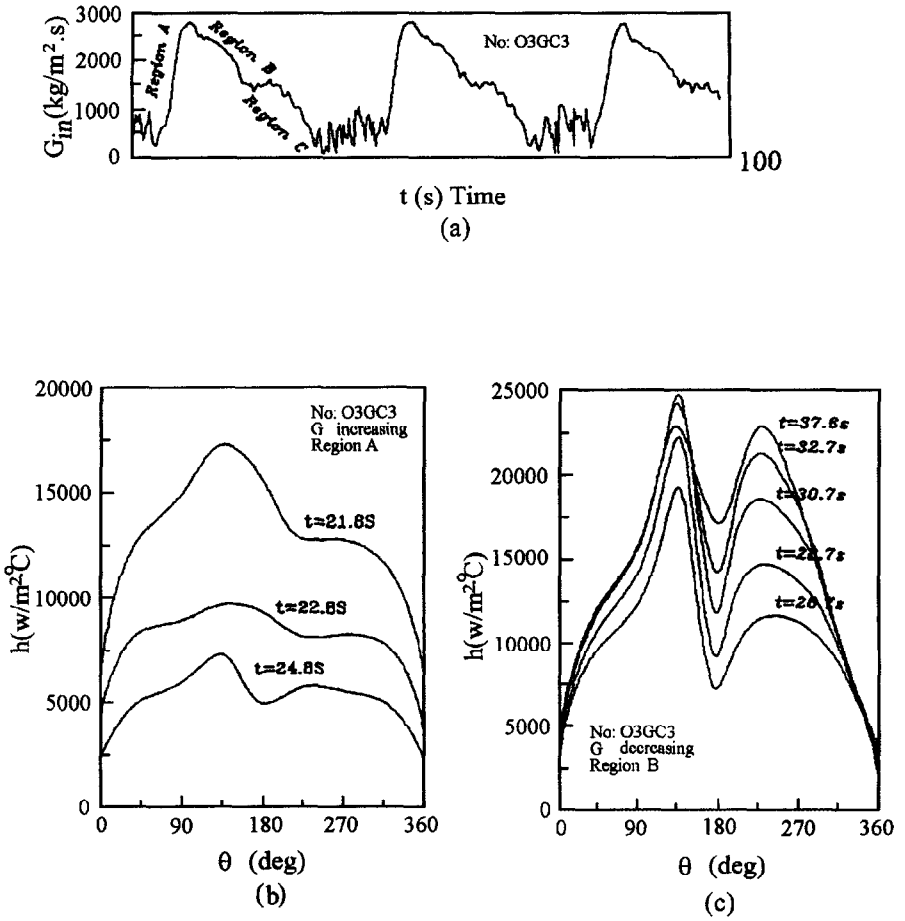

Fig. 9. Transient local heat transfer coefficients variation corresponding to the flow-rate oscillation for single phase turbulent flow.

the process of flow rate increasing, but two peaks during the process of flow rate decreasing as shown in Fig. 9(b) and (c).

These phenomena indicate that the actions and flow patterns of secondary flow in helical coils with oscillatory flow are obviously different from that with steady flow. The secondary flow becomes more complicated, there may exist more than two circulations in a cross-section, and even occurs reverse secondary flow-pattern. The interaction between the flow oscillations and the secondary flow is a very interesting and complicated problem. Further exact investigation is required.

5. Conclusions

(1) Experimental work was performed to investigate the oscillatory heat transfer characteristics of single phase turbulent sub-cooled flow and their phase lag relative to the phase feature of flow-rate oscillations in the ranges of $Re = 25\,000$–$125\,000$, oscillations frequency $f = 0.05$–0.003, which corresponds to the thermal-hydrodynamic oscillations encountered in a helical coiled tube boiling channel.

(2) The cross-sectional average heat transfer at much higher Reynolds number and the non-uniform effects of local heat transfer along the longitudinal and peripheral directions were simultaneously experimentally investigated in steady flow. The average and local heat transfer coefficients can be calculated by equations (12) and (13), respectively. A new phenomenon was observed and analyzed that the effects of secondary flow in curved tubes on heat transfer enhancement weakens contrast to that of turbulent disturbances in the range of much higher Reynolds number.

(3) The time average heat transfer coefficient of single phase turbulent flow under unsteady or oscillatory conditions can be correlated by equation (16). The main factors affecting oscillatory heat transfer include Reynolds number Re, Prandtl number Pr, oscillatory frequency and amplitude, and were ana-

lyzed by introducing two new non-dimensional parameters Wo and A_p defined by equations (14) and (15), respectively.

(4) The transient local heat transfer coefficients oscillate with a reverse phase characteristics in contrast to the flow rate oscillations, and show an asymmetrical and non-uniform feature along the circumferential angle θ, and have one peak in the period of increasing flow rate and two peaks in the period of decreasing flow rate.

Acknowledgements

This work was supported by the National Natural Science Foundation of China. The authors also acknowledge the valuable suggestions and help of Prof. C. F. Ma at Beijing Polytechnic University and Prof. S. Y. Ko at Chinese Academy of Science.

References

[1] Guo LJ, Chen XJ, Bai BF, Feng ZP. Transient heat transfer and critical heat flux in helically coiled tubing steam generators. An invited lecture. In: Proceedings of the 4th World Conference on Experimental Heat Transfer Fluid Mechanics and Thermodynamics, 1997;1:823–9.

[2] Jayanti S, Berthoud G. High-quality dry-out in helical coils. Nucl Eng and Des 1990;1(22):105–18.

[3] Guo LJ. Hydrodynamic characteristics of gas–liquid two-phase flow in horizontal helical coiled tubes. Ph.D. dissertation (in Chinese). China: Xi'an Jiaotong University, 1989.

[4] Nariai H, Kovayashi M, Matsuoka T. Friction pressure drop and heat transfer coefficient of two-phase flow in helically coiled tube once through steam generator for integrated type marine water reactors. Nucl Sci and Tech 1982;19(11):936–47.

[5] Unal HC. Determination of void fraction, incipient point of boiling and initial point of net vapour generation in sodium-heated helically coiled steam generator tubes. Trans ASME J of Heat Transfer 1978;100:268–74.

[6.] Hamakiotes CC, Berger SA. Periodic flows through curved tubes: the effect of the frequency parameter. J Fluid Mech 1990;210:353–70.

[7] Takami T, Sudou K, Sumida M. Pulsating flow in curved pipes. Bull JSME 1984;27:2706–13.

[8] Evans, NA. Heat transfer through the unsteady laminar boundary layer on a semi-infinite flat plate. Int J of Heat Mass Transfer 1973;6:567–80.

[9] Lyne WH. Unsteady viscous flow in a curved pipe. J Fluid Mech 1971;45:13–31.

[10] Chung JH, Hyun JM. Heat transfer from a fully-developed pulsating flow in curved pipes. Int J Heat Mass Transfer 1994;37:42–52.

[11] Zalosh R, Nelson WG. Pulsating flow in a curved tube. J Fluid Mech 1973;59:693–705.

[12] Chow JCF, Li CH. Oscillatory flow in curved tube. ASCE, Engng Mech Speciality Conf. Waterloo Canada, 1976.

[13] Simon HA, Chang MH, Chow JCF. Heat transfer in curved tubes with pulsatile fully developed laminar flow. ASME J Heat Transfer 1977;99:590–5.

[14] Rabadi NJ, Chow JCF, Simon HA. Heat transfer in curved tubes with pulsating flow. Int J Heat Mass Transfer 1982;25(2):195–203.

[15] Havemann HA, Rao NN. Heat transfer in pulsating flow. Nature 1954;174:41.

[16] Roy RP, Yadigaroglu G. An investigation of heat transport in oscillatory turbulent sub-cooled flow. Trans AMSE J of Heat Transfer 1976;98:630–7.

[17] Ito H. Friction factors for turbulent flow in curved pipes. J Basic Engng, Trans ASME. D 1959;81:123–4.

[18] Seban RA, Mclaughlin EF. Heat transfer in tube coils with laminar and turbulent flow. Int J Heat Mass Transfer 1963;6:387–95.

[19] Bai BF, Guo LJ, Chen XJ. A least-squares solution to nonlinear steady-state multi-dimensional IHCP. Int J Thermal and Fluid Science 1997;5(1):39–42.

[20] Bai BF, Guo LJ, Chen XJ. A solution of multi-dimensional transient inverse heat conduction problem using the least-square methods. Journal of Computer Physics (in Chinese), to be published, 1997.

[21] Guo LJ, Feng ZP, Chen XJ. Experimental investigation of forced corrective boiling flow instabilities in horizontal helically coiled tubes. Int J Thermal and Fluid Science 1997;5(3):200–16.

[22] Guo LJ, Feng ZP, Chen XJ. Experimental investigation of pressure drop oscillations of steam-water two phase flow in helically coiled tubing boiler-reactors. Chinese J Eng Thermophysics (in Chinese) 1997;18(2):225–9.

[23] Owhadi A, Bell KJ, Crain B. Forced convection boiling inside helically-coiled tubes. Int J Heat Mass Transfer 1968;11:1779–93.